A simple model for study of sound generation mechanism in mixing layers

by

Lin Zhou, Mingjun Wei and De-Jun Sun

reprinted from

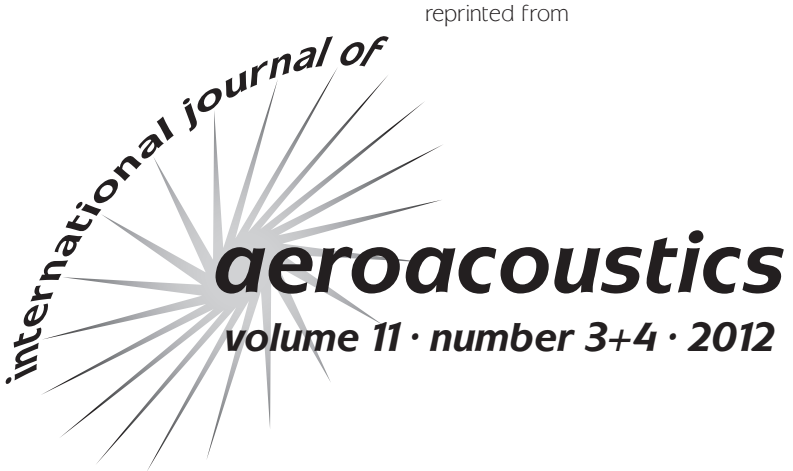

published by MULTI-SCIENCE PUBLISHING CO. LTD.,
5 Wates Way, Brentwood, Essex, CM15 9TB UK
E-MAIL: mscience@globalnet.co.uk
WEBSITE: www.multi-science.co.uk

international journal of aeroacoustics volume 11 · number 3&4 · 2012 – pages 447 – 458

A simple model for study of sound generation mechanism in mixing layers

Lin Zhou[a,b], Mingjun Wei[1,b] and De-Jun Sun[a]

[a]*Department of Modern Mechanics, University of Science and Technology of China, Hefei, P. R. China*
[b]*Department of Mechanical and Aerospace Engineering, New Mexico State University, Las Cruces, U.S.A.*

Submitted: Oct. 1, 2011; Revised: Mar. 8, 2012; Accepted: Mar. 16, 2012

ABSTRACT

Applying Lighthill's acoustic analogy equation to temporally-developing mixing layers, we derived a direct relation between the near-field dynamics, in terms of pressure work, and the far-field sound. The sound radiation predicted by the new model was compared to the direct numerical simulation result, and they agreed well in all stages of vortex dynamics development in mixing layers: roll-up, pairing, merging, saturation, and viscous damping. Using the new formulation, we explained the mechanism for sound generation from the considered flow, and depicted general topological structures for the distribution of sound sources. Though the dynamics is different for vortex roll-up and vortex pairing, the same mechanism for sound generation is suggested by similar topological structures of the sound sources defined here.

1. INTRODUCTION

Noise radiation by free shear flows is one of the most fundamental problems in aeroacoustic community [1–3]. Since Lighthill's pioneer work [4, 5] more than fifty years ago, the acoustic features of shear flows have been studied experimentally [6, 7] and numerically [8–12] in many literatures. It is commonly agreed that there are two types of sound sources existed in subsonic shear layers [7, 13]: 1) large-scale coherent structures (e.g. vortex roll-up and pairing) dominated by instability waves, which produce low-frequency noise; 2) turbulent fine-scale structures, which produce broadband-frequency noise. However, the definition of sound sources is not straightforward in most cases, and it is hard to separate the acoustic features from general hydrodynamic features with their closely-coupled relation. The acoustic analogy first suggested by Lighthill [4] is promising in identifying sound sources by rewriting the Navier-Stokes equations as a wave equation with a lump of source terms.

[1]mjwei@nmsu.edu

Since then, the method has been advanced through many efforts to separate sound sources from the interaction with hydrodynamics [14–18]. Despite great successes of above formulations in their respective applications, it remains hard to provide a simple explanation of sound generation mechanism for most flows.

In this paper, a simple sound source model is derived for temporally-developing mixing layers. The new model reproduces the simulation results accurately in an extremely simple form. More importantly, its simplicity makes possible to explain the sound generation mechanism in a direct manner. In the following sections, we first derive the new model in §2, then describe numerical simulation details for the mixing layer in §3. The comparison between the results from simulation and acoustic analogy is conducted in §4. The same section also includes the discussion (e.g. using topological analysis) of sound generation mechanism for temporally-developing mixing layers. Finally, the conclusion is in §5.

2. ACOUSTIC ANALOGY MODEL

The classical Lighthill's equation [4, 19] is

$$\frac{\partial^2 \rho'}{\partial t^2} - a_\infty^2 \nabla^2 \rho' = \frac{\partial^2 T_{ij}}{\partial x_i \partial x_j}, \tag{1}$$

where the density variation ρ' is described as sound waves being radiated from a nominal source term. The Lighthill's tensor T_{ij} is defined by

$$T_{ij} = \rho u_i u_j - \tau_{ij} + p - \rho a_\infty^2, \tag{2}$$

which includes contributions from the momentum flux tensor $\rho u_i u_j$, the viscous stress τ_{ij}, and the entropy $(p - \rho a_\infty^2)$. With an accurate description of T_{ij}, the sound calculated from (1) is exact. For a temporally-developing mixing layer, Lele et al. [21] suggest that the far-field sound is essentially a plane wave. So that, an average along the streamwise direction (and the spanwise direction for three-dimensional cases) reduces (1) to only one dimension in space,

$$\frac{\partial^2 \langle \rho' \rangle}{\partial t^2} - a_\infty^2 \frac{\partial^2 \langle \rho' \rangle}{\partial y^2} = \frac{\partial^2 \langle T_{yy} \rangle}{\partial y^2}, \tag{3}$$

where $\langle \cdot \rangle$ is the spatial average along x. If we choose an arbitrary observation point (Y, t) at the far field, using Green's function, we can solve the density fluctuation $\rho'(Y, t)$ as an integration of all the contributions from sources at each location y and time t', such as

$$\langle \rho'(Y,t) \rangle = \frac{1}{2a_\infty} \int_{-\infty}^{+\infty} \int_{-\infty}^{t - \frac{|Y-y|}{a_\infty}} \frac{\partial^2 \langle T_{yy}(y,t') \rangle}{\partial y^2} dt' dy. \tag{4}$$

It is noticed that there is a minimum time delay for wave propagation $|Y - y|/a_\infty$. For mixing layers with weak compressibility and a constant temperature, we can neglect the viscous stress term and entropy term from Lighthill's tensor and get $T_{yy} = \rho v^2$.

Applying reciprocal theorem [22], Golanski et al. suggest an acoustic analogy formulation for temporal-developing mixing layers [20],

$$\left\langle \rho'\left(Y,t\right)\right\rangle = \frac{1}{2a_\infty^3}\int_{-\infty}^{+\infty}\frac{\partial}{\partial t'}\left\langle \rho v^2\right\rangle_{t'=t-\frac{|Y-y|}{a_\infty}} dy. \tag{5}$$

The acoustic analogy formulation (5) in its simple form shows that the far field sound is directly determined by the growth rate of perturbation kinetic energy in temporally-developing mixing layers. However, the same as most other formulations, (5) is incapable of explaining the exact mechanism for local events to generate sound. Our intention is to formulate a new model with simple sound sources carrying clear physical meaning, so that, we can easily see the fundamental mechanism of noise generation by mixing layers.

Applying the same assumptions of weak compressibility and constant temperature, we first substitute the density ρ with its mean value $\overline{\rho}$ as it is required for further simplification. As shown in the schematic figure 1, sound sources are expected only in a finite near-field range $[-L_s, +L_s]$, so that, (5) is slightly simplified to

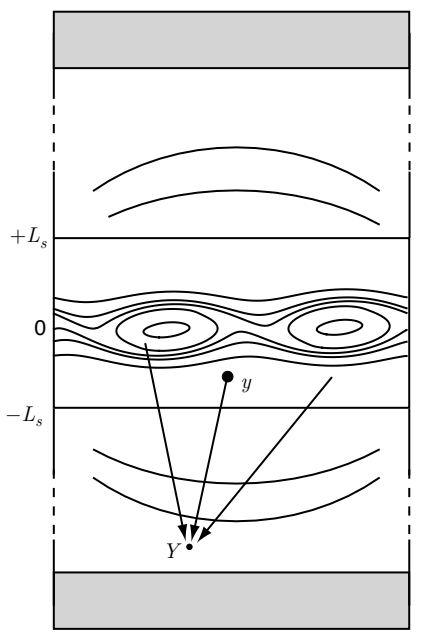

Figure 1: Schematic of the sound generation from temporally-developing mixing layers: the gray areas are computational sponge zones, and sound sources are assumed to reside only between $-L_s$ and $+L_s$.

$$\left\langle \rho'\left(Y,t\right)\right\rangle = \frac{1}{a_\infty^3}\int_{-L_s}^{+L_s}\frac{\partial}{\partial t'}\left\langle \frac{1}{2}\bar{\rho}v^2\right\rangle_{t'=t-\frac{|Y-y|}{a_\infty}} dy. \tag{6}$$

If the distance Y is large comparing to the dimension of the flow field and the wave length [23, 24], we can approximate the time delay factor $|Y-y|/a_\infty$ by $|Y|/a_\infty$, such that,

$$\left\langle \rho'\left(Y,t\right)\right\rangle = \frac{1}{a_\infty^3}\int_{-L_s}^{+L_s}\frac{\partial}{\partial t'}\left\langle \frac{1}{2}\bar{\rho}v^2\right\rangle_{t'=t-\frac{|Y|}{a_\infty}} dy. \tag{7}$$

The growth rate of perturbation kinetic energy $\left\langle \frac{1}{2}\bar{\rho}v^2\right\rangle$ can then be obtained approximately from the order analysis of y-direction momentum equation for general compressible flows,

$$\rho\frac{\partial v}{\partial t}+\rho u\frac{\partial v}{\partial x}+\rho v\frac{\partial v}{\partial y}=-\frac{\partial p}{\partial y}+\left(\frac{\partial \tau_{yx}}{\partial x}+\frac{\partial \tau_{yy}}{\partial y}\right). \tag{8}$$

The flow variables $\mathbf{q}=(\rho,\ u,\ v,\ p)$ can be separated to a parallel base flow $\bar{\mathbf{q}}=(\bar{\rho},\ \bar{U}(y),\ 0,\ \bar{p})$ and a small perturbation $\mathbf{q'}=(\rho',\ u',\ v',\ p')$ as $\mathbf{q}=\bar{\mathbf{q}}+\mathbf{q'}$. Here, only $\bar{U}$ is considered a function of y. Both the pressure and density of the base flow are treated as constants: $\bar{p}=p_\infty$ and $\bar{\rho}=\rho_\infty$. Since there is no y-direction velocity for the base flow, we have $v=v$. Keeping only the first-order terms, we get the perturbation equation,

$$\bar{\rho}\frac{\partial v}{\partial t}+\bar{\rho}\bar{U}\frac{\partial v}{\partial x}=-\frac{\partial p'}{\partial y}+\left(\frac{\partial \tau'_{yx}}{\partial x}+\frac{\partial \tau'_{yy}}{\partial y}\right). \tag{9}$$

Multiplying both sides by v, then, we have

$$\bar{\rho}\frac{\partial}{\partial t}\left(\frac{1}{2}v^2\right)=-v\frac{\partial p'}{\partial y}-\bar{\rho}\bar{U}v\frac{\partial v}{\partial x}+v\left(\frac{\partial \tau'_{yx}}{\partial x}+\frac{\partial \tau'_{yy}}{\partial y}\right). \tag{10}$$

Being averaged along x, it becomes

$$\bar{\rho}\frac{\partial}{\partial t}\left\langle \frac{1}{2}v^2\right\rangle=\left\langle -v\frac{\partial p'}{\partial y}\right\rangle-\left\langle \bar{\rho}\bar{U}v\frac{\partial v}{\partial x}\right\rangle+\left\langle v\left(\frac{\partial \tau'_{yx}}{\partial x}+\frac{\partial \tau'_{yy}}{\partial y}\right)\right\rangle, \tag{11}$$

where $\left\langle \overline{\rho}\overline{U}v\dfrac{\partial v'}{\partial x}\right\rangle$ becomes zero with periodic condition being applied along x. If the viscous effect to acoustics is also neglected here, we end up with a simple equation,

$$\frac{\partial}{\partial t}\left\langle \frac{1}{2}\overline{\rho}v^2\right\rangle = \left\langle -v\frac{\partial p'}{\partial y}\right\rangle. \tag{12}$$

Finally, substituting (12) into (6) and (7), we get two new acoustic analogy models for the far-field sound of temporally-developing mixing layers,

$$AA1: \left\langle \rho'\left(Y,t\right)\right\rangle = \frac{1}{a_\infty^3}\int_{-L_s}^{+L_s}\left\langle -v\frac{\partial p'}{\partial y}\right\rangle_{t'=t-\frac{|Y-y|}{a_\infty}} dy \tag{13}$$

and

$$AA2: \left\langle \rho'\left(Y,t\right)\right\rangle = \frac{1}{a_\infty^3}\int_{-L_s}^{+L_s}\left\langle -v\frac{\partial p'}{\partial y}\right\rangle_{t'=t-\frac{|Y|}{a_\infty}} dy, \tag{14}$$

where $AA1$ is for general source distribution and $AA2$ is for large Y as in (7). The new source term $\langle -v\partial p'/\partial y\rangle$ in $AA1$ and $AA2$ indicates a simple mechanism for sound generation: *The pressure gradient $\partial p'/\partial y$ provides a force of compression or expansion, and such a force together with the same-direction velocity v produces the power term for sound generation. The entire source term can be therefore regarded as localized pressure chambers which work in the same way as of speakers*. There is also engineering convenience from $AA2$: to calculate sound distribution at a fixed time, only a snapshot at an earlier time with spatially-resolved information is required, while most of acoustic analogy models including (5) require both spatially-resolved information (for integration) and temporally-resolved information (for time derivative).

It is noticed that Lighthill has made a similar effort in his earlier work [5] to achieve a simple pressure-related term, which was described as "the product of the pressure and the rate of strain" (see equation (14) in his paper [5]). Among all acoustic analogy models, such a pressure-related term shows the most similarity to our $AA1$ formulation in an ensemble of physical presentation and mathematical simplicity. For comparison, we applied Lighthill's equation (14) of [5] to our setup of temporally-developing mixing layers and obtained the following analogy equation:

$$AAL: \left\langle \rho'\left(Y,t\right)\right\rangle = \frac{1}{a_\infty^3}\int_{-L_s}^{+L_s}\left\langle p'\frac{\partial v}{\partial y}\right\rangle_{t'=t-\frac{|Y-y|}{a_\infty}} dy. \tag{15}$$

Mathematically, the difference between (13) and (15) is that the latter neglects the term $\partial(p'v)/\partial y$, which brings some errors as shown later in the numerical simulation test. Though the above models are all in two-dimensional space, the extension to three-dimensional cases is straightforward with periodic boundary condition being applied along both streamwise and spanwise directions [25].

3. NUMERICAL SIMULATION

The basic configuration of a temporally-developing mixing layer is sketched in figure 1. The Mach number of lower and upper flows are $M_1 = 0.4$ and $M_2 = -0.4$ respectively, and the Reynolds number based on far-field sound speed and initial vorticity thickness is $Re = \rho_\infty a_\infty \delta_\omega/\mu = 500$. The initial flow profile is $U_0 = M_1 + (M_2 - M_1)\mathrm{erfc}(-y)/2$ being super-posed with small perturbations of the most unstable eigenfunctions at the fundamental frequency and its subharmonic frequency, which are both computed from linear instability analysis.

The computational domain along x direction is [0, 26.46] with periodic condition; and it is [−300, 300] along y including large sponge zones at both ends, [−300, −100] and [100, 300]. The near-field region for source integration is $[-L_s, +L_s] = [-30, +30]$. All the lengths are scaled by the initial vorticity thickness δ_ω. Other quantities shown in later figures are also scaled by corresponding characteristic properties without being mentioned again [26]. Spectral method was used for x-direction derivatives, the fourth-order dispersion-relation-preserving scheme [27] was used for derivatives along the y-direction, a fourth-order Runge-Kutta algorithm was used for time advancement. The algorithm and the corresponding code have been extensively validated in our previous works [28–30].

4. RESULTS AND DISCUSSION

First, the results from different models (i.e. $AA1$, $AA2$, and AAL) are compared to the data from direct numerical simulation (DNS). Figure 2 shows the time history of $\langle \rho' \rangle$ at the far field $Y = -90$. Three development stages of far-field sound can be identified according to the development stages of vortex dynamics (with a fixed time delay): stage I – vortex roll-up; stage II – vortex pairing/merging/saturation; stage III – viscous damping. Using DNS data as the benchmark, we plot other four results respectively from Golanski et al.'s formulation (5), $AA1$, $AA2$, and AAL. Overall, the results from all formulations agree well with the DNS result (figure 2a). Four critical moments A, B, C, D are marked in the figure: point A has a fixed time delay $|Y|/a_\infty$ from the moment when the energy of the fundamental frequency reaches the maximum growth rate; point B is $|Y|/a_\infty$ after the first saturation moment when the energy of the fundamental frequency reaches its maximum; point C is $|Y|/a_\infty$ after the moment when the energy of the subharmonic reaches the maximum growth rate; point D is $|Y|/a_\infty$ after the second saturation moment when the energy of the subharmonic reaches its maximum. Physically, points A and B are during the stage of vortex roll-up, and points C and D are during the stage of vortex pairing. When we check the zoom-in details of points A and B (figure 2b), there is a small but consistent difference between DNS and all model results. Apparently, such

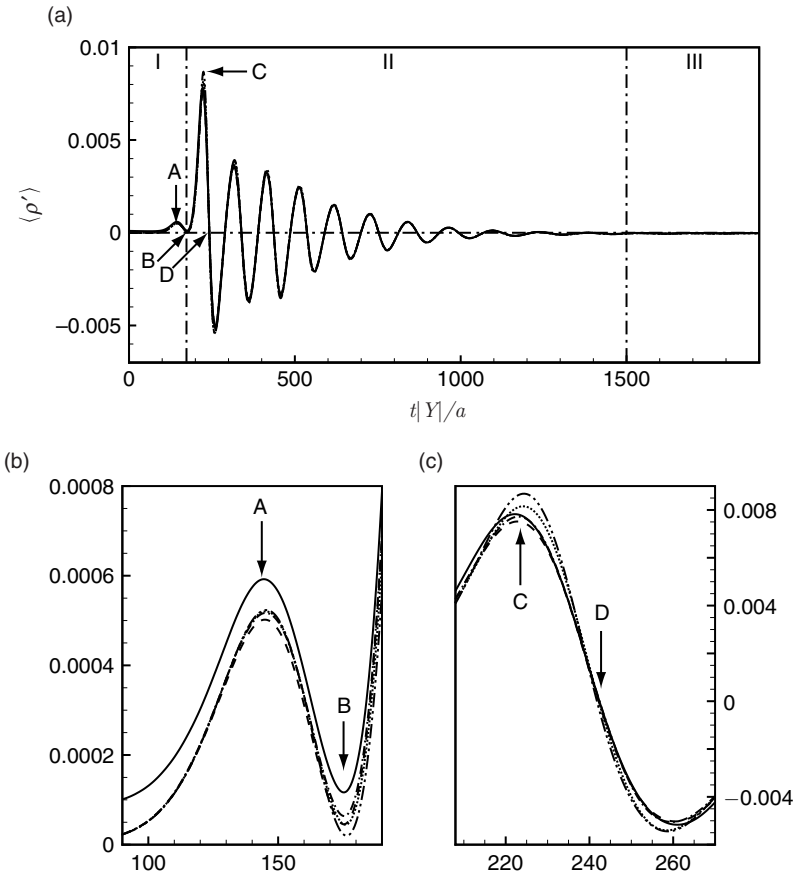

Figure 2: A comparison of the results from DNS (—), Golanski et al.'s model (5) (– –), $AA1$ (– · –), $AA2$ (· · ·), and AAL (– · · –): (a) the time history of $\langle\rho'\rangle$ showing three development stages at the far field $Y = -90$; (b) zoom-in detail of points A and B; (c) zoom-in detail of points C and D.

difference mainly comes from the approximation of removing viscous and entropy terms from Lighthill's tensor in (5) instead of other new assumptions introduced later. Once the vortices are developed (stage II), the effects from viscosity and entropy get smaller, so, the zoom-in details of points C and D (figure 2c) show better agreement. However, for stage II, as the whole mixing area (e.g. shear layer thickness) getting larger, the sound sources distribute in a larger area too. Thus, neglecting the time-delay difference by source distribution in $AA2$ results in a slightly less accurate result. For all points A, B, C, and D, the accuracy of AAL is less than $AA1$ and even $AA2$. This is not to our surprise, since Lighthill's derivation

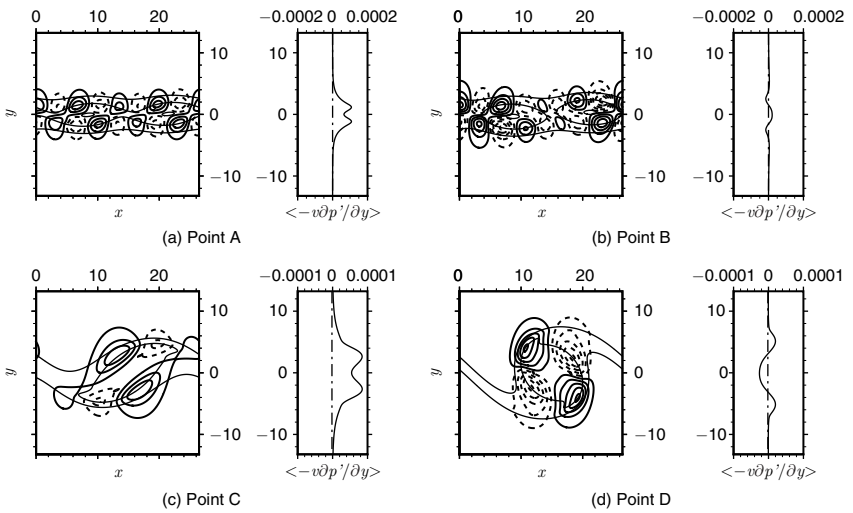

Figure 3: A comparison of the sound source distribution for moments A, B, C, and D. For each moment, the left picture shows $-v\partial p'/\partial y$ with contour levels between $(-0.0012, 0.0012)$ for A and B and $(-0.006, 0.006)$ for C and D; the right picture shows the source term with x-direction integration, $\langle -v\partial p'/\partial y \rangle$. Vorticity contours are marked in thick solid lines for reference purpose.

for AAL [5] has made more aggressive approximation than the current derivation for $AA1$ and $AA2$.

Figure 3 then shows the distribution of the source term $\langle -v\partial p'/\partial y \rangle$ at different time moments A, B, C, and D. It is shown that the sound sources always concentrate near vortices in a small region along y direction. The sources at points A and B are more compact than those at points C and D. This is the reason why $AA2$ can capture the sound more accurately in the stage I than in the stage II. The overall strength of sound sources is stronger in the stage of vortex pairing (i.e. points C and D) than in the stage of vortex roll-up (i.e. points A and B). Within the same stage, the distribution of sound sources is more symmetric for points B and D, therefore, there can be a perfect cancellation of sound. During the whole process of vortex pairing/merging, such symmetric and asymmetric distributions alternate and result in the variation of far-field sound strength in a quasi-periodic manner.

If we decouple the term $-v\partial p'/\partial y$ to its velocity component v and force (pressure gradient) component $\partial p'/\partial y$, as shown in figure 4, the positive and negative velocity components are on the right and left sides of vortices, and the positive and negative force components are instead on the bottom and top sides of vortices. Such a distribution makes the maximum amplitude for the combined term to be at the overlapped corners. This general distribution indicates that any change of velocity or pressure field can result in a change to the higher order combined term at the corners.

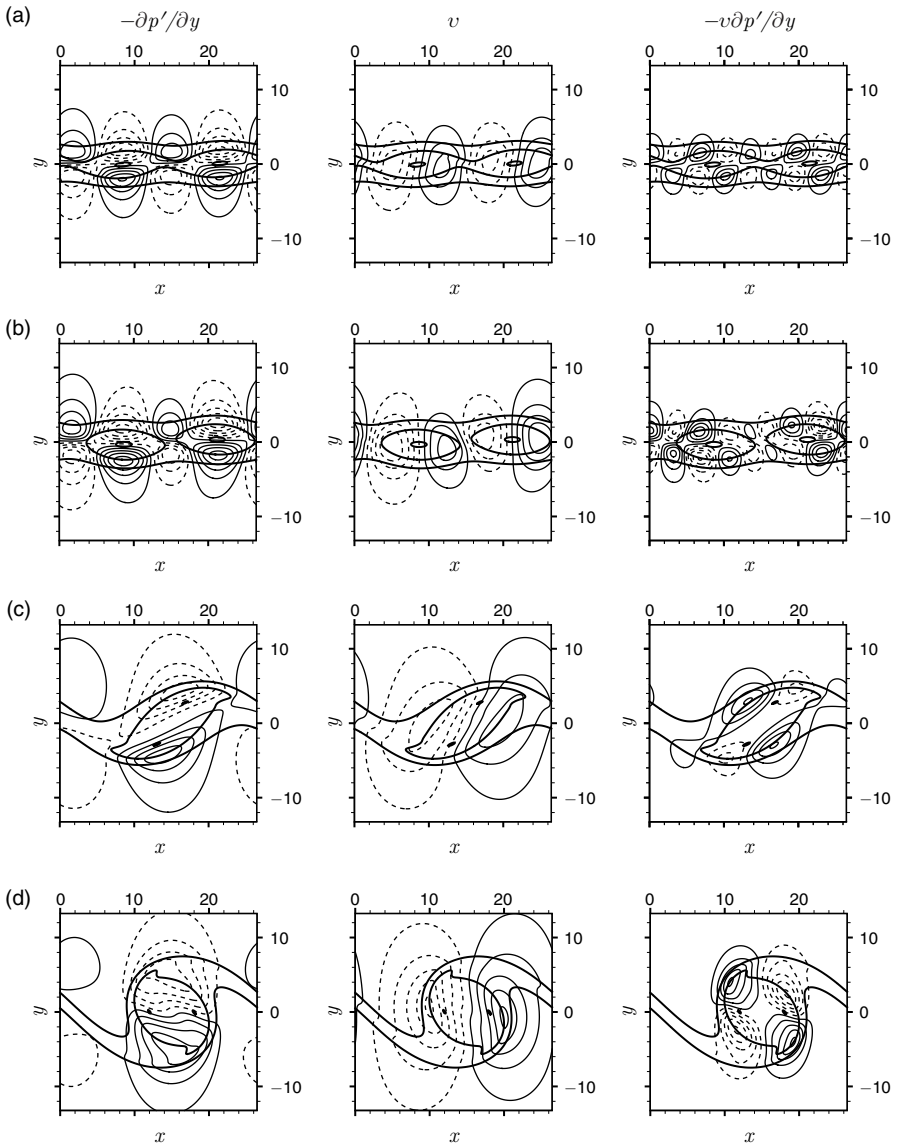

Figure 4: Distributions of force component $-\partial p'/\partial y$, velocity component v, and the combined term $-v\partial p'/\partial y$ for moments A, B, C, and D. For A and B: the contours of $-\partial p'/\partial y$ are between $(-0.015, 0.015)$; the contours of v are between $(-0.15, 0.15)$; the contours of $-v\partial p'/\partial y$ are between $(-0.0012, 0.0012)$. For C and D: the contours of $-\partial p'/\partial y$ are between $(-0.03, 0.03)$; the contours of v are between $(-0.4, 0.4)$; the contours of $-v\partial p'/\partial y$ are between $(-0.006, 0.006)$. Vorticity contours are marked in thick solid lines for reference purpose.

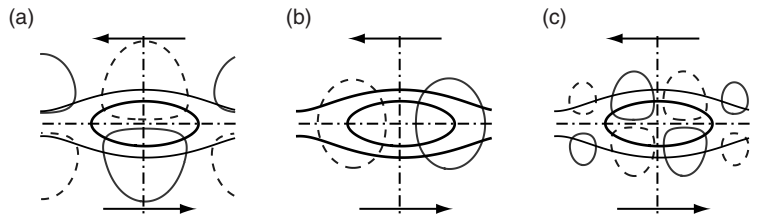

Figure 5: Sketches for general topological structures of: (a) force term $-\partial p'/\partial y$; (b) velocity term v; (c) combined sound source $-v\partial p'/\partial y$. Thin solid and dashed lines are for positive and negative region of corresponding values, thick vorticity contours are marked for reference purpose, and the arrows show the flow directions.

Throughout the entire developing history, the same topological structure exists for the combined source term and the individual components as sketched in figure 5. Such a consistent manner of the local sound source distribution/interaction, even for very distinct dynamic events (e.g. vortex roll-up and pairing), can be a clear indication of the same sound-generation mechanism behind different vortex dynamics in mixing layers.

5. CONCLUSION

In summary, we derived a simple acoustic analogy model for temporally-developing mixing layers. The new model shows a direct connection between the far-field sound and the near-field "work term", which includes the contribution from the y-direction velocity and the pressure gradient along the same direction. The model can accurately predict the far-field sound from a two-dimensional temporally-developing mixing layer. The topological structure depicted in the simple definition of sound sources shows consistent pattern throughout the mixing layer's different developing stages. Such similarity shows the same sound generation mechanism for vortex roll-up and pairing, though their dynamic behavior is distinct.

ACKNOWLEDGEMENT

The authors thank Professor Colonius for the comments and suggestions. LZ and DJS thank the support from National Natural Science Foundation of China (Grant No. 11072238) and 111 Project (Grant No. B07033).

REFERENCES

[1] Goldstein, M. E., "Aeroacoustics of turbulent shear flows," *Annu. Rev. Fluid Mech.*, Vol. 16, 1984, pp. 263–285.

[2] Tam, C. K. W., "Supersonic jet noise," *Annu. Rev. Fluid Mech.*, Vol. 27, 1995, pp. 17–43.

[3] Wang, M., Freund, J. B., and Lele, S. K., "Computational prediction of flow generated sound," *Annu. Rev. Fluid Mech.*, Vol. 38, 2006, pp. 483–512.

[4] Lighthill, M. J., "On sound generated aerodynamically. I. General theory," *Proc. R. Soc. Lond. A*, Vol. 211, 1952, pp. 564–587.

[5] Lighthill, M. J., "On sound generated aerodynamically. II. Turbulence as a source of sound," *Proc. R. Soc. Lond. A*, Vol. 222, 1954, pp. 1–32.

[6] Viswanathan, K., "Aeroacoustics of hot jets," *J. Fluid Mech.*, Vol. 516, 2004, pp. 39–82.

[7] Tam, C. K. W., Viswanathan, K., Ahuja, K. K., and Panda, J., "The source of jet noise: experimental evidence," *J. Fluid Mech.*, Vol. 615, 2008, pp. 253–292.

[8] Colonius, T., Lele, S. K., and Moin, P., "Sound generation in a mixing layer," *J. Fluid Mech.*, Vol. 330, 1997, pp. 375–409.

[9] Mitchell, B. E., Lele, S. K., and Moin, P., "Direct computation of the sound generated by vortex pairing in an axisymmetric jet," *J. Fluid Mech.*, Vol. 383, 1999, pp. 113–142.

[10] Freund, J. B., "Noise sources in a low-Reynolds-number turbulent jet at Mach 0.9," *J. Fluid Mech.*, Vol. 438, 2001, pp. 277–305.

[11] Freund, J. B., "Noise source turbulence statistics and the noise from a Mach 0.9 jet," *Phys. Fluids*, Vol. 15, 2003, pp. 1788–1800.

[12] Colonius, T., "Modeling artificial boundary conditions for compressible flow," *Annu. Rev. Fluid Mech.*, Vol. 36, 2004, pp. 315–345.

[13] Bogey, C. and Bailly, C., "Investigation of downstream and sideline subsonic jet noise using large eddy simulation," *Theor. Comput. Fluid Dyn.*, Vol. 20, No. 1, 2006, pp. 23–40.

[14] Lilley, G. M., "On the noise from jets," *AGARD CP-131.*, 1974.

[15] Goldstein, M. E., "A generalized acoustic analogy," *J. Fluid Mech.*, Vol. 488, 2003, pp. 315–333.

[16] Goldstein, M. E., "On identifying the true sound sources of aerodynamic sound," *J. Fluid Mech.*, Vol. 526, 2005, pp. 337–347.

[17] Sinayoko, S., Agarwal, A., and Hu, Z., "Flow decomposition and aerodynamic sound generation," *J. Fluid Mech.*, Vol. 668, 2011, pp. 335–350.

[18] Cabana, M., Fortune, V., and Jordan, P., "Identifying the radiating core of Lighthill's source term," *Theor. Comput. Fluid Dyn.*, Vol. 22, 2008, pp. 87–106.

[19] Rienstra, S. W. and Hirschberg, A., *An introduction to acoustics*, Eind-hoven University of Technology, 2001.

[20] Golanski, F., Fortune, V., and Lamballais, E., "Noise radiated by a non-isothermal, temporal mixing layer Part II: Prediction using DNS in the framework of low Mach number approximation," *Theor. Comput. Fluid Dyn.*, Vol. 19, No. 6, 2005, pp. 391–416.

[21] Lele, S. K. and Ho, C. M., "Acoustic radiation from temporally evolving free shear layers," *Internal Report. Stanford University.*, 1994.

[22] Howe, M. S., *Theory of vortex sound*, Cambridge University Press, 2003.

[23] Fortune, V., Lamballais, E., and Gervais, Y., "Noise radiated by a non-isothermal,

temporal mixing layer, Part I: Direct computation and prediction using compressible DNS," *Theor. Comput. Fluid Dyn.*, Vol. 18, 2004, pp. 61–81.

[24] Obrist, D., "Directivity of acoustic emissions from wave packets to the far field," *J. Fluid Mech.*, Vol. 640, 2009, pp. 165–186.

[25] Whitmire, J. and Sarkar, S., "Validation of acoustic-analogy predictions for sound radiated by turbulence," *Phys. Fluids*, Vol. 12, No. 2, 2000, pp. 381–391.

[26] Wei, M., *Jet noise control by adjoint-based optimization*, University of Illi-nois at Urbanan-Champaign, 2004.

[27] Tam, C. K. W. and Webb, J. C., "Dispersion-relation-preserving finite difference schemes for computational acoustics," *J. Comput. Phys.*, Vol. 107, No. 2, Aug 1993, pp. 262–281.

[28] Wei, M. and Freund, J. B., "A noise-controlled free shear flow," *J. Fluid Mech.*, Vol. 546, 2006, pp. 123–152.

[29] Wei, M. and Rowley, C. W., "Low-dimensional models of a temporally evolving free shear layer," *J. Fluid Mech.*, Vol. 618, 2009, pp. 113–134.

[30] Cavalieri, A. V. G., Jordan, P., Gervais, Y., Wei, M., and Freund, J. B., "Intermittent sound generation and its control in a free-shear flow," *Phys. Fluids*, Vol. 22, 2010, pp. No. 115113.